・ステロイド依存例
　ステロイド漸減中の再燃

登録状況（目標症例30例）
　ステロイド抵抗例(n=1)，ステロイド依存例（n=3）

患者背景
　年 齢　：38.7歳（28-47）
　性（M/F）：2/2
　病　型：全大腸炎型　2
　　左側大腸炎型　2
　罹病期間：　6.7年（6-7）
　入院回数：　4回（3-5）

[方法]
・投与方法
　全大腸炎型
　　デキサメサゾン封入ポリ乳酸マイクロカプセル（DxMC）840mg/day（デキサメサゾン1mgを含有）を、4週間隔日経口投与
　左側大腸炎型
　　DxMC 840mg/dayを4週間隔日注腸投与

・治療評価
　投与前、2週後、4週後
　1．臨床スコア（CAI）
　2．大腸内視鏡所見
　3．血液・生化学・尿

[中間結果]
・ステロイド依存例　有効　26歳　男性　左側大腸炎型　DxMC注腸投与
　投与前に下降結腸からS状結腸にかけて深掘れ潰瘍があったが、投与4週後、殆ど潰瘍が消失し、瘢痕状態になった。
・ステロイド依存例　（効果不明）　47歳　男性　大腸炎型　DxMC経口投与
　ステロイド減量のリバウンド、CMV感染を合併したため、このカプセル自体の効果は不明となった。
・ステロイド抵抗例では殆ど効果を認めなかった。

[結果のまとめ]
1. 難治性潰瘍性大腸炎患者4例に、DxMCを投与した。
2. DxMCの効果
　ステロイド抵抗患者：　効果を認めなかった
　ステロイド依存患者：　2例で有効　1例で効果不明
　マイクロカプセル自体の明らかかな副作用はなかった
3. DxMCはステロイド依存患者に良い適用と考えられた。
　今後も症例を蓄積し、DxMCの有効性と安全性を検討する

II. リポ化ステロイドを用いたドラッグデリバリーシステムによる炎症性腸疾患の治療：多施設共同による無作為化並行群間試験

[パルミチン酸デキサメサゾン（リメタゾン）の特性]

・現在、本邦で市販されている薬剤としてはパルミチン酸デキサメサゾン、製品名リメタゾンがある。
・特性
　・デキサメタゾンをパルミチン酸エステルとして脂溶性を高め、ダイズ油に溶解した乳濁製注射液である。
　・炎症部への分布が高く、炎症部マクロファージに積極的に貪食され、そのマクロファージの中で溶解し、マクロファージ機能を効率よく抑制する。従って、薬剤投与量の軽減化により、副作用が軽減される。
　※リメタゾン：慢性関節リウマチで保険適用で市販
　　通常2週間に1度投与で、副腎機能の抑制はない

[研究課題]

・リポ化ステロイドを用いたドラッグデリバリーシステムによる炎症性腸疾患の治療・多施設共同による無作為化並行群間試験（関西医科大学医学倫理委員会　第0635号　承認）

[目的]

・炎症性腸疾患（潰瘍性大腸炎、クローン病、腸管型ベーチェット病）患者におけるリポ化ステロイドによるドラッグデリバリーシステムの有用性を検討する

[対象]

・活動期炎症性腸疾患（重症例は除く）
　潰瘍性大腸炎、クローン病、腸管型ベーチェット病
・ステロイド依存例
　従来の全身的ステロイド剤投与が有効であるが漸減中に再燃する患者

[登録状況]（目標症例数30例）

・潰瘍性大腸炎（n=1）クローン病（n=1）腸管型ベーチェット（n=2）

[方法]

・疾患別に下記治療法を無作為化

[治療法]

① 従来の全身的ステロイド剤投与量を再増量
② 従来の全身的ステロイド剤投与量は変更なく、更にリメタゾン1管（1ml）を1ヶ月間週1回投与し、以後の2ヶ月間は2週毎に1回投与
　⇒リメタゾン投与量（プレドニゾロン換算）
　　投与開始前1ヶ月間は2.2mg/日、以後の2ヶ月間は1.1mg/日にあたる
　3ヵ月間施行し2週毎に有効性を評価
　⇒投与開始2週後
　有効：従来の全身的ステロイド剤の投与量を減量
　無効：他の治療法に変更

[治療評価]

・投与前、2週後、4週後、6週後、8週後、10週後、12週後
　1. 臨床スコア
　2. 血液（CRP、血沈、生化学）
　3. 内視鏡所見（2週後、4週後、12週後）
　4. 従来の全身的ステロイド剤の投与量変化
　5. ステロイド剤の副作用
　6. リメタゾンの副作用の有無

[Primary endpoint]

治療の有効性：臨床スコア・血液（CRP・赤沈）・内視鏡所見のうち2項目以上の改善・軽快を有効とする。

[Secondary endpoint]
従来の全身的ステロイド剤の減量が可能であったか、副作用が軽減
[投与・観察スケジュール]
・最初の1ヶ月間は毎週、それ以後は2週毎に投与　3ヶ月間で8回投与
・2週毎に臨床スコアを検討
・内視鏡所見は4回（投与時、2週、4週、12週
[症例]
・潰瘍性大腸炎　38歳　男性　ステロイド依存例　プレドニン20mg投与⇒12週後　10mgに減量　有効
・腸管型ベーチェット病　53歳　男性　大きな潰瘍あり　投与前プレドニン15mg、イムラン50mg
服用中止60週でも悪化なし　有効例
[結語のまとめ]
1. ステロイド依存性の炎症性腸疾患患者3例にリメタゾンを投与した。
潰瘍性大腸炎患者で2例　クローン病1例　腸型ベーチェット2例　計4例に投与
2. リメタゾンの効果
潰瘍性大腸炎：有効　ステロイドの減量が可能であった。
クローン病：現在投与中（初回投与後10日）
腸管型ベーチェット：　有効　ステロイドの中止が可能であった。
明らかなリメタゾンの副作用はなかった。
3. 今後も症例を蓄積（目標症例30例）し、リメタゾンの有効性と安全性と検討する。
今後も症例登録にご協力をお願いします。

＜質疑応答＞
班長：ヒトへの臨床応用というところに視点をおいて研究を進めている。難治例ということもあり患者選択が難しい。最初の薬剤は院内製剤であり、外には出せないが、リメタゾンは費用的にやすく（一人分がトータルで2万円位）、当班は終了するが、是非参加をお待ちいたします。症例が集まれば何らかの形で文献化したいと考えている。

◎ 新しいコンセプトによる治療法開発（15：50～16：20）

11）OPC-6535の腸管NK細胞とクローン病を中心とした腸炎抑制機序について（研究分担者：日比紀文）
○ 高山哲朗[1]、岡本　晋[1]、井上 詠[1]、市川仁志[2]、鎌田信彦[1]、知念 寛[3]、北爪美奈[1]、
小林　拓[1]、斎藤理子[1]、久松理一[1]、金井隆典[1]、日比紀文[1]
（[1]慶應義塾大学医学部消化器内科、[2]東京歯科大学市川総合病院消化器科、[3]琉球大学医学部付属病院光学医療診療部）

[OPC-6535 Drug Data]
・炎症性腸疾患、閉塞性呼吸器疾患の領域で開発中の新規チアゾール誘導体
・好中球のスーパーオキサイド産生を抑制する薬剤としてScreeningされた。
・作用機序は完全に解明されていないが、その作用の一部はPDE4阻害による。
・サイトカインやホルモンなどの刺激が受容体に結合すると2次蛋白を介してATPからcAMPが生成される。このcAMPがPKAなどの活性などを通じて遺伝子発現関与する。PDE4は数あるPDEの中の免疫担当細胞において高発現しているもので、cAMPを分解するものである。
・OPC-6535はPDE4を抑制することで、cAMP濃度を高め、それによって作用を発現すると考えられている。

・OPC6535 はヒト単球からの TNF-αや IL-12 産生抑制効果を示した。
・EARK、p38、p65、STAD3 については OPC-6535 投与群においてもリン酸化への影響は認めなかった。
・PKA 費依存性の経路で効果を示すことが示唆された。
・IL=10 ノックアウトマウスの自然腸炎発症を抑制した
・他の PDE 4 阻害剤や cAMP アナログとの作用効果及び機序の差異は見出せなかった。

【OPC6535 の他の免疫担当細胞への効果】
・T 細胞の効果： TNFα、INFγ産生に対して抑制が見られる。
・NK 細胞への効果： 濃度依存的に INFγ産生が抑制されることから抗炎症効果を持つ

【炎症性腸疾患、腸管手術検体での OPC の効果の検討】

◆免疫担当細胞は抹消血中と腸管局所では機能が異なることが報告されていることから、それに対する検討
◆クローン病腸管 NK 細胞での検討を進めているので OPC でも解析を実施
【背景】
・我々はクローン病において腸管の NK 細胞が健常者や UC と比べて増加していることを確認している。
・免疫染色：クローン病の腸管では INFγを多く産生する NK 細胞が増えていることが示唆された。
・クローン病の腸管から LPM を単離し、CD3 と CD56 で展開すると、もともと INFγのメジャーソースとして T 細胞が知られているが、サイトカイン（IL-12）刺激で INFγを産生する。同時に腸管の NK 細胞からも INFγが出てくることがわかった。
・菌（死菌）刺激でも NK 細胞からも INFγがたくさん出てくることがわかった。

【OPC の効果】
・サイトカインで刺激した場合
クローン病の腸管から LPM をとってきて、未刺激の状態では INFγは出ていないが、IL-12, 15 の刺激により、殆どの細胞が INFγを亢産生するが、OPC を加えると濃度依存性に抑制されることが確認された。
cAMP でも同様に下がるが、その作用はかなり弱い。
・菌刺激の場合
菌刺激の場合も同様に腸管の NK 細胞から INFγが出てくるが、OPC を加えると濃度依存性に抑制されることが確認された。

・腸管の T 細胞に対する検討
サイトカイン刺激に対して出てくる INFγを OPC は濃度依存的に抑制することが確認された。
菌刺激に対しても同様であった。
【まとめ】
・OPC6535 は末梢血中の T 細胞、NK 細胞からの免疫性サイトカイン産生を抑制する。
・クローン病では、腸管の NK 細胞が増加しており、commensal bacterial 刺激により著明に炎症性サイトカインを産生する。
・OPC6535 および cAMP analogue はクローン病の腸管 NK 細胞、腸管 T 細胞に対しても炎症性サイトカイン産生を濃度依存性に抑制する。

＜質疑応答＞
Q:OPC6535 はコードネームか？
A:一般名はテトミラスト。

Q:この薬剤は腸管の上皮にはどのように働くか?cAMP を上げるということは、上皮を増殖したり、下痢の原因になったりする可能性は?
A:その検討はしていない。
Q:マクロファージに対してはどうか?
A:マクロファージからの IL-23 の産生も抑制している。
Q:開発の状況は?
A:米国で潰瘍性大腸炎の有効性が乏しくかったが、その後の解析ではクローン病で期待されている。

12) 新規ケモカイン CXCL16 制御を目的とした炎症性腸疾患に対する治療開発　(研究分担者:千葉　勉)
○ 仲瀬裕志、宇座徳光、千葉　勉 (京都大学大学院医学研究科消化器内科学)

【Pathophysiology of IBD】
・バクテリアが関係している。
・APC, DC, 活性化したマクロファージ、T 細胞が暴れだすと悪さをするということで、いろんなターゲットがあるが、IL-17, HGF などの増殖因子など、
・我々がターゲットとしたものは APC をメインにするものであり、DDS をすればよくなる。

【SR-PSOX/CXCL16】
・2000 年にスカベンジャーレセプターとして発見された　と同時に CXCCR6 のリガンドとして同定された膜結合型のケモカインである。
・脳と骨格筋以外の臓器に広く分布する。
・消化管ではパイエル板のみに発現
・血球成分ではマクロファージと DC に発現
・4 つの domain を有する膜結合型で発現する。
・スカベンジャーレセプター
ケモカインレセプターはバクテリアをファゴサイトするファンクションを有している。
樹状細胞、マクロファージのところに CXCL16 が出ており、バクテリアが取り込まれる。また、
Tcell、CXCCR6 がリガンドとくっついて、interaction をおこす。こういった interaction により、炎症の継続や生体のホメオスターシスを保っていると考える。

【目的】
実験腸炎モデルを用いて SR-PSOX/CXCL16 の役割を検討する。
※preliminary な段階で患者血清を見たところ、UC/CD とも CXCL16 は上がっている。

【実験デザイン】※実際に炎症を起こして、上がっているのかを見た
Mice　:CXCL16　10−12 適齢、メス、SPF 環境下
Induction of colitis :3% DSS　M.W.36000-50000
検討項目:
・腸炎誘導前後の大腸組織における CXCL16 の発現を解析 (real time PCR 法)
・蛍光免疫染色による CXCL16　発現細胞とその分布の検討 (今回はまだ confirm していない)
結果:
大腸組織における CXCL16 の発現

炎症をおこすと、CXCL16の発現はあがることが確認された。

⇒【CXCL16は腸炎発症に関わっているのか?】

ノックアウトマウスで検討（DSSを用い）

[経時的体重変化]

・ノックアウトマウスではnormalと比べて体重変化が軽微であった。

[腸管長の比較]

・マクロで見てもノックアウトの方が腸管長は非常に長い wild typeとノックアウトを比較すると有意差があり、炎症はコントロール出来ているのではと考えられた。

[組織学的評価]

・wild typeとノックアウトを比べてみると大腸に関してはphenotypeは差が出なかった。

・DSSをもちいるとWild typeでは炎症細胞浸潤がかなり強くでるが、ノックアウトではクリプトは残りある程度はブロックできるが完治したとまでは行かない。組織学的スコアは差がある。

※DSSのモデルでCXCL16をノックアウトすると炎症は軽くなることが示唆された。

[大腸組織におけるサイトカインの発現]

・TNF-α、IL-1B、INF-γは下がるが、IL-10は上がることを予想したが、炎症が下がればカウンターでIL-10も下がるという結果であった。

【まとめ】

・CXCL16は腸炎の発症に関与していることが判明した。

【実験的腸炎モデルにおいてCXCL16は治療のターゲットになりうるか?】

・ヒトでの検討が必要であり、抗体を作って検討した

・予防的な投与で、DSSを入れる前から投与する。

体重変化：6日前後で変わってくる、もう少しみると差がでる。

腸管長：コントロールIgGとCXCL16の抗体では有意差が出る。

組織学的評価：CXCL16抗体群は完全ではないがクリプトが保たれており、組織像は改善している。

※CXCL16の抗体をつくってブロッキングすると腸炎が改善するデータが得られた。

別なモデルで検討

⇒TNBS腸炎で検討 SJL miceを使用

CXCL16の抗体をもちいて検討

体重変化：3〜4日で差が出てくる。

組織学的評価：コントロールと比べるとCXCL16の抗体ではクリプトが戻ってくる

※現在はIL-10KOと掛け合せて、検討中である。

【ヒトでの検討】

・CXCL16をヘルシーコントロール、活動期CD,非活動期CD、活動期UC,非活動期UC,で見ると2つとも上がっていた。

・疾患の活動性ととCXCL1を見ると相関関係が示唆された。

・白血球除去療法でみると、UCのリスポンダーでは下がり、ノンリスポンダーでは変わらないことが確認されたので、治療のマーカーにも使えることが示唆された。

【まとめ】

・CXCL16は腸炎発症に関与していると考えられた。

・CXCL16は病気のマーカーとして使えることが示唆された。

＜質疑応答＞

Q: CXCL16の阻害剤は？

A:抑える薬剤はない。

Q:治療に生かすのは？

A:抗体療法の可能性はある。

事務局連絡

平成20年度スケジュール

平成21年

2月　6日（金）　平成20年度　第2回総会

2月　8日（金）　分担研究者報告書類提出　締め切り

総合研究報告書18年度～20年度

※昨年11月の事後評価報告書を若干変更してもらえれば良い。

3月　6日（金）　収支決算報告書提出　締め切り

IX. 研究成果の刊行物・別刷

Involvement of Smad3 phosphoisoform-mediated signaling in the development of colonic cancer in IL-10-deficient mice

DAISAKU HACHIMINE[1], KAZUSHIGE UCHIDA[1], MASANORI ASADA[2], AKIYOSHI NISHIO[2], SEIJI KAWAMATA[1], GO SEKIMOTO[1], MIKI MURATA[1], HIDEO YAMAGATA[1], KATSUNORI YOSHIDA[1], SHIGEO MORI[1], YOSHIYA TAHASHI[1], KOICHI MATSUZAKI[1] and KAZUICHI OKAZAKI[1]

[1]Third Department of Internal Medicine, Kansai Medical University, Moriguchi, Osaka;
[2]Department of Gastroenterology, Graduate School of Medicine, Kyoto University, Kyoto, Japan

Received February 7, 2008; Accepted March 19, 2008

Abstract. Chronic inflammation predisposes to cancer. Transforming growth factor (TGF)-ß, a multifunctional protein, suppresses the growth of normal colonic epithelial cells, whereas it stimulates the proliferation of cancer cells. Interleukin (IL)-10-deficient mice, which develop colitis and colorectal cancer, show an increased level of plasma TGF-ß. Although TGF-ß may be a key molecule in the development of colon cancer arising from chronic colitis in IL-10-deficient mice, the role of TGF-ß still remains unclear. TGF-ß activates not only TGF-ß type I receptor (TßRI) but also c-Jun N-terminal kinase (JNK), which converts the mediator Smad3 into two distinctive phosphoisoforms: C-terminally phosphorylated Smad3 (pSmad3C) and linker-phosphorylated Smad3 (pSmad3L). We studied C57BL/6-IL-10-deficient mice (n=18) at 4 to 32 weeks of age. We investigated histology, and pSmad2/3L, pSmad2/3C, and p53 by immunohistochemistry. pSmad3L staining was detected in the cancer cells in all 10 mice with colonic cancer and in the epithelial cells in 7 of 12 mice with colonic dysplasia, but not in the normal or colitic mice. pSmad3c was detected without any significant difference between stages. p53 was weakly stained in a few cancer cells in 5 out of 10 mice. Smad3L signaling plays an important role in the carcinogenesis of chronic colitis in IL-10-deficient mice.

Introduction

In 1925, Crohn and Rosenberg documented a case of rectal carcinoma complicating ulcerative colitis (UC) and postulated that the lesion developed as a late manifestation of the disease (1), and many subsequent epidemiological studies have confirmed this increased risk (as high as 34%) after 25 years of disease (2). In contrast to sporadic colorectal cancers, which develop through the 'adenoma-carcinoma sequence', inflammatory bowel disease (IBD)-associated carcinomas develops through the 'dysplasia sequence'. Although cancers from UC as well as sporadic colorectal carcinoma are hypothesized to arise from a multistep process, the precise mechanism is still unknown.

Interleukin (IL)-10-deficient mice under specific-pathogen free conditions spontaneously develop chronic enterocolitis, a condition phenotypically similar to chronic IBD in humans (3). An increase in the incidence rate of colorectal carcinoma has been observed in conjunction with elevated plasma transforming growth factor (TGF)-ß1 levels at 10 to 31 weeks of age (4), which suggests that TGF-ß may be a key molecule in the development of colon cancer arising from chronic colitis in IL-10-deficient mice. Therefore, this murine IBD model may provide excellent insights into the pathogenetic mechanism of chronic colitis-associated carcinoma.

TGF-ß is a multifunctional protein that regulates a complex array of cellular processes, including proliferation, differentiation, motility, and death in a cell-specific manner (5). TGF-ß can inhibit colonic epithelial cell growth, acting as a tumor suppressor (6) and also plays a major role in the negative regulation of immune cell functions, particularly in the gut (7). Loss of TGF-ß (8) or unresponsiveness to TGF-ß1 (9) in the colonic epithelium has been associated with the development or progression of inflammation in the colon. However, increased TGF-ß activity may be involved in tumor development rather than tumor suppression in IL-10-deficient mice (5). The role of TGF-ß in tumor development thus seems to be dual, and dependent on the stage of the tumor. These multiple functions are thought to result from different intracellular signaling pathways. Recent evidence suggests that TGF-ß is also a key regulator of epithelial-to-mesenchymal transition (EMT) in cell phenotypes (10). EMT not only underlies epithelial degeneration and fibrogenesis in chronic degenerative disorders, but also endows dedifferentiated malignant epithelial cells with mesenchymal, migratory, and proteolytic properties that are required for local tumor invasiveness (11). Inhibition of the pro-inflammatory cytokine IL-1ß at initiation of EMT has been

Correspondence to: Dr Kazuichi Okazaki, Third Department of Internal Medicine, Kansai Medical University, 10-15 Fumizono-cho, Moriguchi, Osaka, 570-8506, Japan
E-mail: okazaki@hirakata.kmu.ac.jp

Key words: Smad3, colonic cancer, interleukin-10

found to attenuate fibrogenesis (12), suggesting a causative link between chronic inflammation and EMT. The main downstream signaling pathway for TGF-ß involves the Smad proteins (13). Although several studies of EMT have suggested that the process involves Smad-independent pathways (14), recent studies using Smad3 knockout mice have indicated that signaling through the Smad3-dependent pathway is required for injury-dependent multistage transition of an epithelial cell to a mesenchymal phenotype (15). Therefore, we focused on Smad3 signaling (16,17), and on the different roles of Smad3 phosphoisoform-mediated signaling in epithelial cells and mesenchymal cells, reported recently (18). Thus, TGF-ß activates not only TGF-ß type I receptor (TßRI) but also c-Jun N-terminal kinase (JNK), converting Smad3 into two distinct phosphoisoforms: C-terminally phosphorylated Smad3 (pSmad3C) and linker-phosphorylated Smad3 (pSmad3L). The TßRI/pSmad3C pathway inhibits growth of epithelial cells, while JNK/pSmad3L-mediated signaling promotes ECM deposition by activated mesenchymal cells such as hepatic stellate cells (HSCs) (5). However, it is unclear how Smad3 signaling is involved in the development of colon cancer during long-standing chronic colitis.

In the present study, according to these phosphorylation-defined activities, we studied whether Smad3 phosphoisoforms govern progression from chronic colitis to colonic cancer in an IL-10-deficient mouse model.

Materials and methods

Animals. C57BL/6-IL-10-deficient mice (aged 4-32 weeks) were purchased from The Jackson Laboratory (Bar Harbor, ME). The animals were housed under specific-pathogen free (SPF) conditions and fed autoclaved food and sterile water in the animal facility of the Graduate School of Medicine, Kyoto University. Of these, the IL-10-deficient mice were transferred from SPF to conventional housing conditions at six weeks of age as they spontaneously develop colitis under conventional housing conditions by eight weeks of age. All animal experiments were performed in accordance with our institutional guidelines.

Histology. The entire large intestines were examined in 18 IL-10-deficient mice between 4 and 32 weeks of age. The large intestines were fixed in 4.5% buffered formaldehyde before embedding in paraffin blocks. For histological analysis, 5-μm sections were cut and stained with hematoxylin and eosin (H&E). The principal histologic distinction was between dysplasia and colorectal carcinoma according to Japanese criteria. Histologic slides involving diagnoses of normal, dysplasia and adenocarcinoma were reviewed independently by two pathologists specialising in gastrointestinal neoplasia.

Domain-specific Abs against the phosphorylated Smad3. Polyclonal anti-phospho-Smad3 antibodies [anti-pSmad3L ($Ser^{207/212}$) and anti-pSmad3C ($Ser^{423/425}$)] were raised against the phosphorylated linker regions and COOH-terminal regions of Smad3 by immunization of rabbits with synthetic peptides. The relevant antisera were affinity purified with the phosphorylated peptides as described previously (16).

Table I. Serial analysis of intestines in IL-10-deficient mice.

Age (weeks)	n	Colitis	Dysplasia	Cancer
4	3	0	0	0
7	1	1	0	0
8	2	2	2	0
12	2	2	2	1
16	2	2	2	2
24	2	2	2	2
28	4	4	4	4
32	2	2	2	2

Immunohistochemistry. Immunohistochemical staining was performed on formalin-fixed, paraffin-embedded tissue sections. The sections were deparaffinized in xylene, and rehydrated in graded alcohols. Antigen retrieval was done by microwave irradiation in 0.01 M sodium citrate buffer (pH 6.0) for 15 min. After cooling, the endogenous peroxidase activity was blocked by incubation in 3% H_2O_2 in methanol for 10 min. After rinsing with TBS containing 0.1% Tween-20 (TBST), non-specific antigens were blocked by preincubation with 1% bovine serum albumin (Nakarai, Kyoto, Japan). The sections were incubated overnight with the following primary antibodies: anti-mouse p53 (1.0 μg/ml, Abcam, Cambridge, UK), anti-pSmad3L (1.0 μg/ml) and anti-pSmad3C (1.0 μg/ml). After rinsing with TBST, the sections were incubated with peroxidase-labeled polymer conjugated to goat anti-rabbit immunoglobulin for 1 h at room temperature. The peroxidase activity was visualized with 3,3'-diaminobenzidine (Vector Laboratories, Burlingame, CA) counterstained with Mayer's hematoxylin (Merck, Darmstadt, Germany), and mounted under coverslips. The evaluation of immunoreactivity was performed by microscopy (Olympus BX 50, Tokyo, Japan). Immunohistochemistry was scored by pathologists in double-blind fashion according to staining proportions as follows: 0, no staining seen; 1, staining seen in 5-30% of cells; 2, staining seen in >30% of cells.

Statistical analysis. Statistical evaluation was done using the nonparametrical Mann-Whitney U ranking test. Values were based on two-tailed statistical analysis.

Results

Development of colorectal dysplasia and carcinomas in IL-10-deficient mice. We confirmed a previous report that IL-10-deficient mice develop colitis after 7 weeks. We found that mice developed dysplasia or cancer after 8 to 12 weeks, respectively (Table I; Fig. 1). We observed no metastasis in the mesenteric lymph nodes or liver in any mice. We also observed that the small intestine was not affected.

Smad3 phosphorylation of COOH-terminals and linker regions. Immunohistochemical analysisis was performed on mice from each stage to detect Smad3 phosporylation. pSmad3C was detected without significant difference between

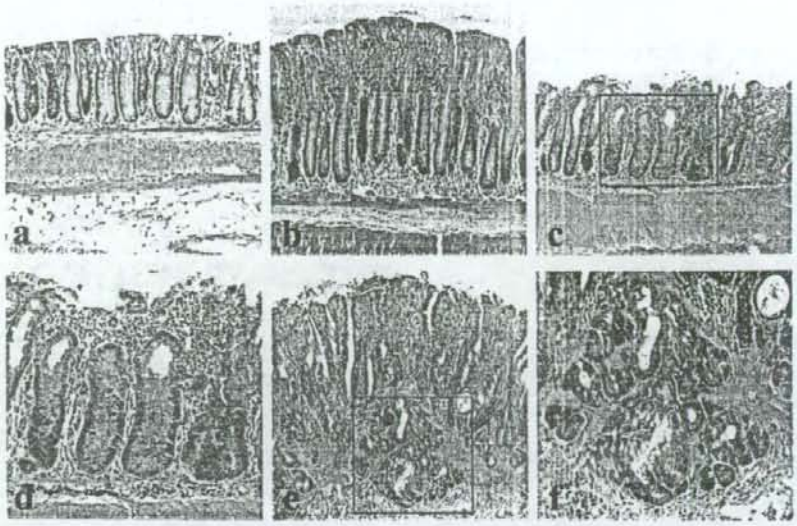

Figure 1. Histopathological findings of the colorectum in IL-10-deficient mice using hematoxylin and eosin staining (H&E). Normal colonic mucosa (a, x40). IL-10-deficient mice developed colitis (b, x40) after 7 weeks. Dysplasia (c, x40; d, x200) and cancer (e, x40; f, x200) were found after 8-12 weeks.

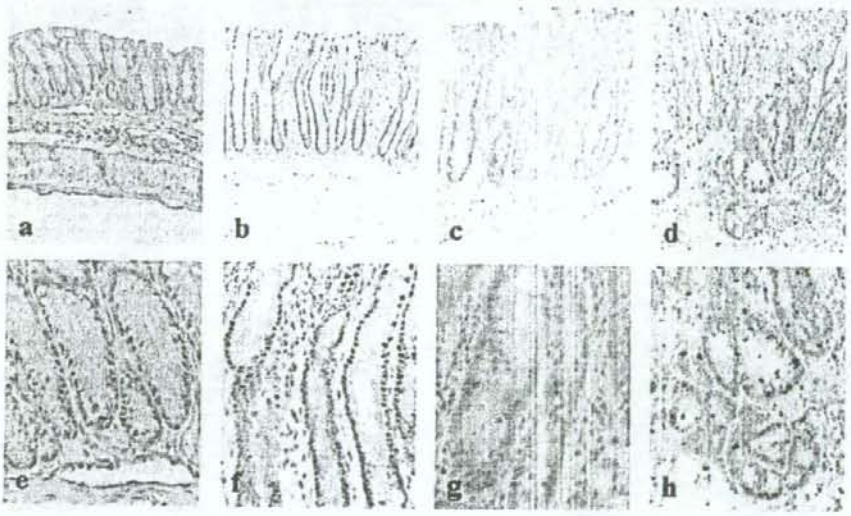

Figure 2. Immunohistochemical findings of the colorectum in IL-10-deficient mice using anti-pSamd3C antibody. pSmad3C was detected without significant difference between stages. Normal mucosa (a, x40; e, x200); colitis (b, x40; f, x200); dysplasia (c, x40; g, x200); cancer (d, x40; h, x200).

stages (Figs. 2 and 5). On the other hand, pSmad3L detection levels gradually increased from dysplasia to adenocarcinoma (Figs. 3 and 5). pSmad3L was expressed in dysplasia and cancer cells, but not in inflamed mucosa cells, even in the mice with cancer.

p53 expression in colorectal cancers. To determine p53 expression, all mice were subjected to immunohistochemical analysis using rabbit anti-mouse p53 polyclonal antibody. p53 was detected only in the mice with colonic cancer (Figs. 4 and 5). Dysplasia of the colorectal epithelium was not stained with anti-p53 antibody (Figs. 4 and 5). In 5 out of the 10 mice with cancer, the cancer cells were stained, however very few cells were p53 positive and even so stained weakly (Figs. 4 and 5).

Discussion

Colon cancer in patients with ulcerative colitis is thought to be associated with long-standing tissue injury and chronic inflammation (19). The relationship between chronic inflammation and cancer dates back to Virchow, who, in

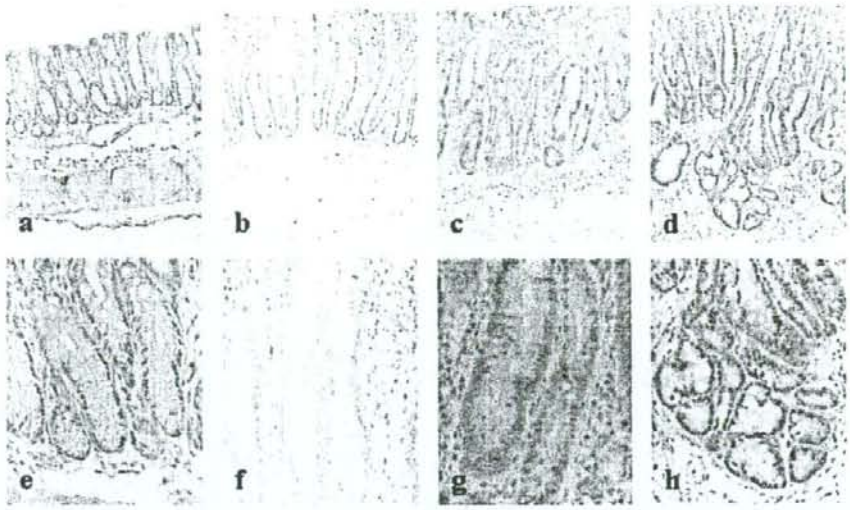

Figure 3. Immunohistochemical findings of the colorectum in IL-10-deficient mice using anti-pSamd3L antibody. pSmad3L detection levels gradually increased from dysplasia to adenocarcinoma. Normal mucosa (a, x40; e, x200); colitis (b, x40; f, x200); dysplasia (c, x40; g, x200); cancer (d, x40; h, x200).

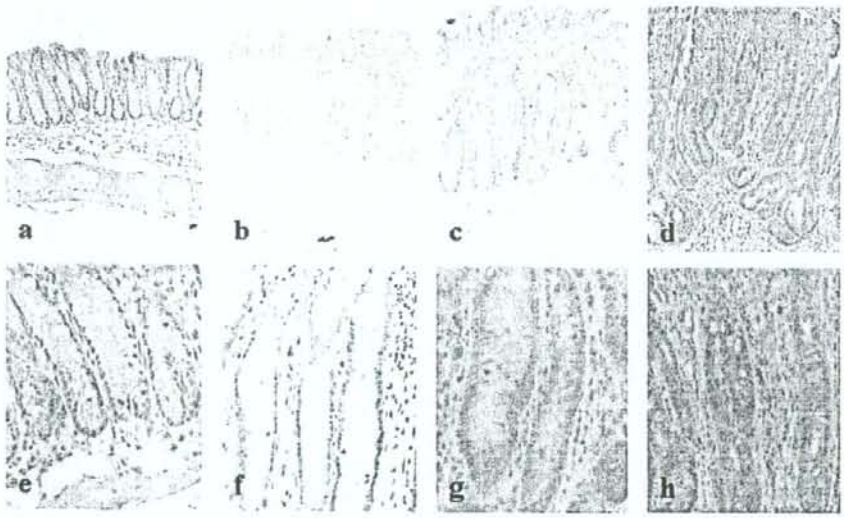

Figure 4. Immunohistochemical findings of the colorectum in IL-10 deficient mice using anti-p53 antibody. In 5 out of 10 mice with cancer, a few cancer cells were stained weakly. Normal (a, x40; e, x200); colitis (b, x40; f, x200); dysplasia (c, x40; g, x200); cancer (d, x40; h, x200).

1863, hypothesized that the origin of cancer was at sites of chronic inflammation (20). Although the relation between chronic inflammation and cancer has been well established in general, the molecular mechanisms involved in the process remain unclear. Certainly, chronic inflammation leads to increased oxidative stress. Leukocytes and other phagocytic cells generate reactive oxygen and nitrogen species, which, in turn, can damage proliferating epithelial cells. Also, chronic inflammation appears to promote the apoptosis of normal epithelial cells which can lead to a compensatory proliferative response by the remaining tissue.

Our present study confirmed that IL-10-deficient mice, spontaneously develop colonic dysplasia and cancer at a high rate following chronic colitis (4). In IL-10-deficient mice, it has been shown that serum levels of TGF-ß1 significantly increase in mice with dysplasia and cancer, compared to those without tumors (4). This led us to a hypothesize that genetic alterations in other members of the TGF-ß receptor signal transduction pathway are involved in the development of colon cancer in long-standing colitis. TGF-ß, which can potently inhibit epithelial cell growth to act as a tumor suppressor (10), is also a key regulator of epithelial-to-

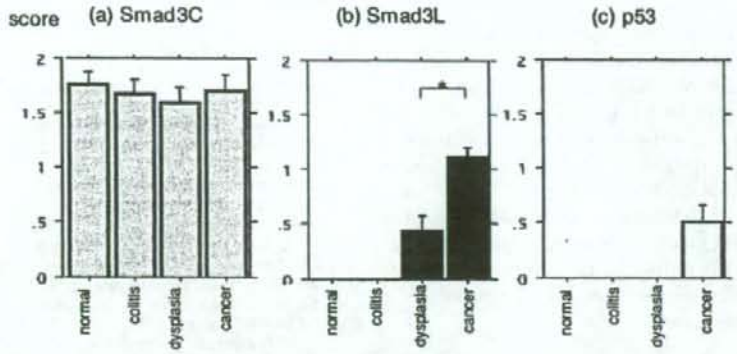

Figure 5. Immunohistochemical scores of Smad3C, 3L and p53. Immunohistochemistry was scored by pathologists in double-blind fashion according to staining proportions as follows: 0, no staining seen; 1, staining seen in 5 to 30% of cells; 2, staining seen in >30% of cells. pSmad3L detection levels increased significantly from colitis to dysplasia (0.417±0.513) to adenocarcinoma (1.100±0.316) ($p<0.05$). In normal and inflamed mucosa, even in cancerous mice, pSmad3L was not detected. Cancer cells were also stained with p53, however very few cells were positive and even so stained weakly (0.500±0.527). pSmad3C was detected without any significant difference between stages. Scores of pSmad2C staining in normal mucosa, colitis, dysplasia, and cancer were: 1.750±0.452, 1.667±0.492, 1.583±0.515, and 1.700±0.483, respectively.

mesenchymal transition (EMT) in cell phenotypes. EMT may be related to the loss of tumor responsiveness on the growth inhibitory effect of TGF-ß and at the same time to the TGF-ß-induced angiogenesis, and local and systemic immunosuppression. During carcinogenesis, tumors show EMT, thereby becoming insensitive to TGF-ß-mediated growth inhibition while showing increased tumor invasion and metastasis (10,21).

TGF-ß signaling is initiated when this ligand induces the formation of a heteromeric complex composed of TGF-ß receptor type I (TßRI) and type II (TßRII). This allows TßRII to phosphorylate TßRI, which then transmits the signal through phosphorylation of receptor-regulated Smads (R-Smads) such as Smad2 and Smad3 (22). R-Smads are directly phosphorylated at COOH-terminal SXS regions by TßRI and then undergo formation of heteromeric complexes with Smad4 (23). Activated Smad complexes are then translocated into the nucleus, where they regulate the expression of target genes both by direct DNA binding and through interaction with other transcription factors, co-activators, and co-repressors (24). Smads contain two highly conserved domains, the Mad homology 1 (MH1) and 2 (MH2) domains, which are connected by interposed linker regions (25). Although the MH1 domains can interact with DNA, the MH2 domains are endowed with transcriptional activation properties (23). In human colorectal cancer, somatic mutation of the Smad4 (18q21) or Smad2 gene (18q21) has been detected in the MH2 domain, but mutations of Smad3 (15q21), Smad6 (15q21), and Smad7 (18q21) genes have not been detected so far (26). On the other hand, Smad3-deficient mice develop colorectal carcinoma (27). Although several studies of EMT have suggested that the process involves Smad-independent pathways (23), there is evidence from Smad3-deficient mice that signaling through the Smad3-dependent pathway is required for injury-dependent multistage transition of an epithelial cell to a mesenchymal phenotype (15). As a consequence, we have focused on Smad3 signaling (16,17) and successfully developed polyclonal antibodies, which specifically recognize the phosphorylated linker regions and phosphorylated COOH-terminal SXS regions of Smad3 (17). Using these antibodies, we recently reported that Smad3 phosphorylated at linker regions or COOH-terminal regions existed as separate molecules with different functions and transmitted distinct signals (16-18). We also previously reported that as neoplasia progresses from normal colorectal epithelium through adenoma to invasive adenocarcinoma with distant metastasis, nuclear pSmad3L gradually increases while pSmad3C decreases (28). The TßRI/Smad pathway is widely represented in most cell types and tissues studied to date, and additional pathways are activated following cell stimulation by TGF-ß in specific contexts. The most prominent pathways are mediated by the mitogen activated protein kinase (MAPK) family, which consists of the extracellular signal-regulated protein kinase pathways c-Jun NH2-terminal kinase (JNK) and p38 pathways (29). TGF-ß induces activation of MAPK pathways through the upstream mediators Ras, RhoA, PP2A, and TGF-ß-activated kinase I (17). Thus, TGF-ß activates not only TßRI but also JNK, which converts Smad3 into two distinctive phosphoisoforms: pSmad3C and pSmad3L (5). Therefore, during sporadic human colorectal carcinogenesis, the shift from TßRI/pSmad3C-mediated to JNK/pSmad3L-mediated signaling is a major mechanism orchestrating a complex transition of TGF-ß signaling (5).

In the present animal study, we observed a significant increase in pSmad3L as neoplasia progressed from normal colorectal epithelium through dysplasia. Our study showed that, unlike human sporadic colon cancer, there were no changes in the phosphorylation of pSmad3C in the murine model. Moreover, no mice showed deep invasion and metastasis of cancer, which suggested that the malignant potential might be low in IL-10-deficient colitis.

The p53 mutation is known as the most common cancer-related genetic change (30). The overexpression of p53 occurs frequently in ulcerative colitis-associated colorectal carcinoma regardless of stage and pathological characteristics (31). In our results, p53 could only be detected in

some cancerous cells, and positive staining was weak. These findings, together with previous reports suggest that *p53* mutations are unlikely to be involved in the malignant transformation of epithelial cells in mice (4). Also, inactivation of *p53* may occur in the late stages of colorectal cancers developing in IL-10-deficient mice, thus being present in only a small number of tumor cells and barely detectable by the methods used in our study.

In conclusion, the phosphorylation of Smad3L may play an important role in the carcinogenesis of colorectal cancer associated with chronic colitis in IL-10-deficient mice. Further studies in human ulcerative colitis are necessary for the clarification of colitic cancer.

Acknowledgements

This study was partly supported by Grants-in-Aid for scientific program (C) from the Ministry of Science and Culture of Japan (18590755), and by Grants-in-Aid from the Health, Labor and Welfare Ministry of Japan.

References

1. Crohn BB and Rosenberg H: The sigmoidscopic picture of chronic ulcerative colitis (non-specific). Am J Med Sci 170: 220-228, 1925.
2. Kewenter J, Ahlman H and Hulten L: Cancer risk in extensive ulcerative colitis. Ann Surg 188: 824-828, 1978.
3. Reninick DM, Fort MM and Davidson NJ: Studies with IL-10-/- mice; an overview. J Leukoc Biol 61: 389-396, 1997.
4. Strulan S, Oberhuber G, Beinhauer BG, Tichy B, Kappel S, Wang J and Rogy MA: Interleukin-10-deficient mice and inflammatory bowel disease associated cancer development. Carcinogenesis 22: 665-671, 2001.
5. Matsuzaki K and Okazaki K: Transforming growth factor-beta during carcinogenesis: the shift from epithelial to mesenchymal signaling. J Gastroenterol 41: 295-303, 2006.
6. Moses HL, Yang EY and Pietenpol JA: TGF-beta stimulation and inhibition of cell proliferation: new mechanistic insights. Cell 63: 245-247, 1990.
7. MacDonald TT: Effector and regulatory lymphoid cells and cytokines in mucosal sites. Curr Top Microbiol Immunol 236: 113-135, 1999.
8. Maloy KJ and Powrie F: Regulatory T cells in the control of immune pathology. Nat Immunol 2: 816-822, 2001.
9. Eppert K, Scherer WS, Ozcelik H, *et al*: MADR maps to 18q21 and encodes a TGF-ß-regulated MAD-related protein that is functionally mutated in colorectal carcinoma. Cell 86: 543-552, 1996.
10. Zavadil J and Bottinger EP: TGF-ß and epithelial-to-mesenchymal transitions. Oncogene 24: 5764-5774, 2005.
11. De Caestecker MP, Piek E and Roberts AB: Role of transforming growth factor-ß signaling in cancer. J Natl Cancer Inst 92: 1388-1402, 2000.
12. Kolb M, Margetts PJ, Anthony DC, *et al*: Transient expression of IL-1beta induces acute lung injury and chronic repair leading to pulmonary fibrosis. J Clin Invest 107: 1529-1536, 2001.
13. Heldin CH, Miyazono K and ten Dijke P: TGF-ß signaling from cell membrane to nucleus through SMAD proteins. Nature 390: 465-471, 1997.
14. Derynck R and Zhang YE: Smad-dependent and Smad-independent pathways in TGF-ß family signaling. Nature 425: 577-584, 2003.
15. Saika S, Kono-Saika S, Ohnishi Y, *et al*: Smad3 signaling is required for epithelial-mesenchymal transition of lens epithelium after injury. Am J Pathol 164: 651-663, 2004.
16. Furukawa F, Matsuzaki K, Mori S, *et al*: p38 MAPK mediates fibrogenic signal through Smad3 phosphorylation in rat myofibroblasts. Hepatology 38: 879-889, 2003.
17. Mori S, Matsuzaki K, Yoshida K, *et al*: TGF-ß and HGF transmit the signals through JNK-dependent Smad2/3 phosphorylation at the linker regions. Oncogene 23: 7416-7429, 2004.
18. Yoshida K, Matsuzaki K, Mori S, *et al*: Transforming growth factor-ß and platelet-derived growth factor signal via c-Jun N-terminal kinase-dependent Smad2/3 phosphorylation in rat hepatic stellate cells after acute liver injury. Am J Pathol 166: 1029-1039, 2005.
19. Ekbom A, Helmick C, Zack M and Adami HO: Ulcerative colitis and colorectal cancer. A population-based study. N Engl J Med 323: 1228-1233, 1990.
20. Balkwill F and Mantovani A: Inflammation and cancer: back to Virchow? Lancet 357: 539-45, 2001.
21. Oft M, Peli J, Rudaz C, Schwarts H, Beug H and Reichmann E: TGF-beta1 and Ha-Ras collaborate in modulating the phenotypic plasticity and invasiveness of epithelial tumor cells. Genes Dev 10: 2462-2477, 1996.
22. Shi Y and Massague J: Mechanisms of TGF-beta signaling from cell membrane to nucleus. Cell 113: 685-700, 2003.
23. Derynck R and Zhang YE: Smad-dependent and Smad-independent pathways in TGF-beta family signaling. Nature 425: 577-584, 2003.
24. Kretschmar M, Doody J, Timokhina I and Massague J: A mechanism of repression of TGFbeta/Smad signaling by oncogenic Ras. Genes Dev 13: 804-816, 1999.
25. Robinson MJ and Cobb MH: Mitogen-activated protein kinase pathways. Curr Opin Cell Biol 9: 180-186, 1997.
26. Miyaki M and Kuroki T: Role of Smad4 (DPC4) inactivation in human cancer. Biochem Biophys Res Commun 306: 799-804, 2003.
27. Zhu Y, Richardson JA and Parada LF: Smad3 mutant mice develop metastatic colorectal cancer. Cell 94: 703-714, 1998.
28. Yamagata H, Matsuzaki K, Mori S, *et al*: Acceleration of Smad2 and Smad3 phosphorylation via c-Jun NH2-terminal kinase during human colorectal carcinogenesis. Cancer Res 65: 157-165, 2005.
29. Mulder KM: Role of Ras and Mapks in TGFbeta signaling. Cytokine Growth Factor Rev 11: 23-35, 2000.
30. Vogelstein B: Cancer. A deadly inheritance. Nature 348: 681-682, 1990.
31. Harpaz N, Peck AL, Yin J, *et al*: p53 protein expression in ulcerative colitis-associated colorectal dysplasia and carcinoma. Hum Pathol 25: 1069-1074, 1994.

Subcutaneous Adipose Tissue–Derived Stem Cells Facilitate Colonic Mucosal Recovery from 2,4,6-Trinitrobenzene Sulfonic Acid (TNBS)–Induced Colitis in Rats

Yugo Ando,[*†] *Muneo Inaba,*[*‡§] *Yutaku Sakaguchi,*[*†] *Masanobu Tsuda,*[*] *Guo Ke Quan,*[*] *Mariko Omae,*[*] *Kazuichi Okazaki,*[†‡§] *and Susumu Ikehara*[*†§]

Background: Adipose tissue–derived stem cells (ADSCs) can be easily obtained from subcutaneous adipose tissue, and ADSCs can be demonstrated to display multilineage developmental plasticity. In this study, using TNBS-induced colitis rats, we show the feasibility of repairing injured intestinal mucosa with adipose tissue–derived stem cells.

Methods: The subcutaneous adipose tissue of F344 rats was obtained and digested by collagenase. The digested tissue was cultured in DMEM containing 10% FBS for 1 month. ADSCs were confirmed to differentiate under appropriate conditions into various lineages of cells, including bone, neural cells, adipocytes, and epithelial cells. HGF, VEGF, TGF-β, and adiponectin in the culture supernatants of ADSCs were determined by ELISA. ADSCs (10^7 cells) were injected into the submucosa of the colon to examine their capacity to repair intestinal mucosa injured by TNBS.

Results: In the experimental colitis model, the injection of ADSCs facilitated colonic mucosal repair and reduced the infiltration of inflammatory cells. High levels of HGF, VEGF, and adiponectin were detected in the culture supernatants of ADSCs. Moreover, injected ADSCs distributed to several layers of the colon, and some of them differentiated into mesodermal lineage cells.

Conclusions: ADSCs can accelerate the regeneration of injured regions in experimental colitis. HGF, VEGF, and adiponectin might be responsible for the regeneration of injured regions in the colon.

(Inflamm Bowel Dis 2008;14:826–838)

Key Words: HGF, VEGF, adiponectin, subcutaneous adipose tissue, Crohn's disease

Crohn's disease is characterized by chronic relapsing inflammation of the gastrointestinal tract. Evidence suggesting that various immune, genetic, and environmental factors influence both the initiation and progression of colitis has been accumulated. However, the precise mechanism or mechanisms underlying the development of this disease have yet to be clarified.

In recent years, several groups have reported the ubiquitous distribution of adult stem cells in various tissues and organs, including bone marrow, muscle, brain, skin, and, more recently, even in subcutaneous fat.[1] Among these adult stem cells, those in the subcutaneous fat, termed adipose tissue–derived stem cells (ADSCs), can be easily obtained with a relatively lower burden on donors; they can be easily harvested from subcutaneous adipose tissue by lipoaspiration. These ADSCs have been demonstrated to display multilineage developmental plasticity.[2] Furthermore, ADSCs have been reported to have less heterogeneity in their immunophenotype and multilineage differentiation ability[3,4] than do bone marrow–derived mesenchymal stem cells. Because of these advantages, clinical use of ADSCs for not only fat, bone, and myocardium reproduction but also spinal cord regeneration, vascularization, and the treatment of intractable ulcers has been carried out, and the development of further clinical applications is expected. Garcia-Olmo et al[5] reported in a phase I clinical trial of Crohn's disease that after an operation to close fistula, cell therapy using autologous ADSCs can facilitate fistula repair. However, ADSCs may have, in general, a potential to treat Crohn's disease and inflammatory bowel disease (IBD) in addition to the treatment for fistula

Received for publication August 10, 2007; accepted December 4, 2007.

From the *First Department of Pathology, Kansai Medical University, Osaka, Japan; †Third Department of Internal Medicine, Kansai Medical University, Osaka, Japan; ‡Regeneration Research Center for Intractable Diseases, Kansai Medical University, Osaka, Japan; and §Center for Cancer Therapy, Kansai Medical University, Osaka, Japan.

Supported by a grant from Haiteku Research Center of the Ministry of Education; a grant from the Millennium program of the Ministry of Education, Culture, Sports, Science and Technology; a grant from the Science Frontier program of the Ministry of Education, Culture, Sports, Science and Technology; a grant from the 21st Century Center of Excellence (COE) program of the Ministry of Education, Culture, Sports, Science and Technology; a grant from the Department of Transplantation for Regeneration Therapy (sponsored by Otsuka Pharmaceutical Company, Ltd.); a grant from Molecular Medical Science Institute, Otsuka Pharmaceutical Co., Ltd.; a grant from Japan Immunoresearch Laboratories Co., Ltd. (JIMRO); and by Grant-in-Aid for inflammatory bowel disease of the Ministry of Health, Labor and Welfare.

Reprints: Susumu Ikehara, Kansai Medical University, Pathology, Osaka, Japan (e-mail: ikehara@takii.kmu.ac.jp)

DOI 10.1002/ibd.20382

Published online 5 February 2008 in Wiley InterScience (www.interscience.wiley.com).

observed in a subpopulation of patients with Crohn's disease. Therefore, the potential ability of ADSCs to improve mucosal healing of inflammatory lesions and the biological mechanism underlying the repair function of ADSCs should be examined. In the present study, using Crohn's disease models in rats in which the colonic mucosa is injured by TNBS, we attempted to treat the mucosal injury by a submucosal injection of ADSCs to facilitate mucosal recovery; we expected this to be a simple and safe procedure. It is noted that ADSCs injected intravenously might be trapped by the reticuloendothelial system in the liver or lung[6]; therefore, they could not be recruited to the intestinal mucosa. Thus, in this study, ADSCs were directly injected into the submucosa, and ADSCs actually facilitated the regeneration of the injured region (by TNBS injection). Furthermore, we also examined the potency of ADSCs to differentiate into various lineage cells and their production of growth factors such as HGF, VEGF, TGF-β, and adiponectin that may accelerate mucosal regeneration.

MATERIALS AND METHODS

Animals

F344/DuCrlCrlj rats were purchased from Charles River Laboratories Japan, Inc. (Yokohama, Japan), and maintained for 1 to 2 weeks in our animal facilities before the start of TNBS treatment. Rats were maintained on a 12-hour light/12-hour dark cycle under pathogen-free conditions and had a standard diet and water until reaching the desired age (13 weeks).

Isolation and Culture of Rat Subcutaneous Adipose Tissue–Derived Stem Cells (ADSCs)

The subcutaneous adipose tissue of F344 rats was obtained by abdominal incision. The raw subcutaneous adipose tissue was washed extensively with sterile phosphate-buffered saline (PBS; Gibco, Invitrogen Corporation, Carlsbad, Calif.) to remove blood cells. The extracellular matrix was digested with a solution of type II collagenase (0.075%; Gibco, Invitrogen Corporation, Carlsbad, Calif.) in balanced salt solution (5 mg/mL; Gibco, Invitrogen Corporation, Carlsbad, Calif.) for 60 minutes at 37°C to release the cellular fraction.[5] Next, the collagenase was inactivated by the addition of an equal volume of RPMI (Sigma-Aldrich, St. Louis, Mo.) containing 10% fetal bovine serum (FBS; Invitrogen Corporation, Carlsbad, Calif.). The suspension of cells was centrifuged at 250g for 10 minutes. Cells were resuspended in DMEM (Sigma-Aldrich, St. Louis, Mo.) plus 10% FBS. The mixture was centrifuged at 250g, and the cells were resuspended in DMEM plus 10% FBS and a 1% ampicillin/streptomycin mixture (Sigma-Aldrich, St. Louis, Mo.) and then were plated in a 75-cm^2 flask (BD Biosciences, Bedford, Mass.) at a concentration of 10–15 $\times$ 10^3 cells/cm^2. Cells were cultured for 24 hours at 37° in an atmosphere of 5% CO_2 in air. Then the dishes were washed with PBS to remove nonadherent cells and cell fragments. The cells were maintained in culture in the same medium and under the same conditions until they reached approximately 80% confluence, with replacement of the culture medium every 3 to 4 days. Cells were then passaged with 0.05% trypsin-EDTA (Gibco, Invitrogen Corporation, Carlsbad, Calif.) at a dilution of 1:3. We used these cells (between passages 1 and 3) as ADSCs for transplantation, and characterization of ADSCs was performed using cells at passages 1 to 3. Furthermore, doubling time was determined by manually counting the number of cells.

In Vitro Differentiation of ADSCs

Adipogenic Differentiation

Adipogenic differentiation was performed by the method previously described by Lee et al[4] with slight modifications. To induce adipogenic differentiation, ADSCs were seeded at a density of 10^4 cells/cm^2 in 8-chamber slides (Nunc, Inc., Naperville, Ill.) and cultured in α-MEM (Nacalai Tesque, Kyoto, Japan) + 10% FBS until reaching 100% confluence; thereafter, the cells were further cultured for 21 days in the presence of 1 μM dexamethasone (Sigma-Aldrich, St. Louis, Mo.), 5 μg/mL recombinant human insulin (Wako Pure Chemical Industries, Ltd., Osaka, Japan), and 4.5 g/L glucose (Wako Pure Chemical Industries, Ltd., Osaka, Japan), as reagents for adipogenic differentiation. The cells cultured without these reagents (α-MEM + 10% FBS alone) served as a negative control. Adipogenic differentiation was confirmed by the formation of neutral lipid vacuoles stained with Oil Red O (Wako Pure Chemical Industries, Ltd., Osaka, Japan). For the Oil Red O stain, cells were fixed with 10% formalin, washed, and stained with a working solution of 0.18% Oil Red O for 5 minutes. The nuclei were counterstained with Mayer's hematoxylin solution (Wako Pure Chemical Industries, Ltd., Osaka, Japan).

Osteogenic Differentiation

To promote osteogenic differentiation, ADSCs were seeded at a density of 1 $\times$ 10^4 cells/cm^2 in 8-chamber slides and cultured in DMEM + 10% FBS until they reached 70% to 80% confluence. Osteogenic differentiation of ADSCs was induced by culturing them for 4 weeks with the osteogenic induction medium, which consisted of 0.1 μM dexamethasone (Sigma-Aldrich, St. Louis, Mo.), 10 mM β-glycerophosphate (Sigma-Aldrich, St. Louis, Mo.), and 0.2 mM ascorbate (Sigma-Aldrich, St. Louis, Mo.).[7] The cells cultured without these reagents (DMEM + 10% FBS alone) served as a negative control. Osteogenic differentiation was confirmed by the increased expression of alkaline phosphatase (ALP) by histochemical staining (TRACP & ALP double-stain kit; TAKARA BIO, Otsu, Shiga, Japan) and also by von Kossa

staining determining the deposition of the hydroxyapatite matrix.

Neural Differentiation

Neural differentiation of ADSCs was carried out according to the method described elsewhere (Woodbury et al, 2000).[8] Briefly, subconfluent ADSCs (70%–80% confluence) were cultured for 24 hours in preinduction medium [DMEM, 20% FBS, 1 mM β-mercaptoethanol (Wako Pure Chemical Industries, Ltd., Osaka, Japan)], and the cells were further incubated in the neurogenic medium (NM), which consisted of DMEM and 10 mM β-mercaptoethanol.[9] Neural differentiation was immunohistochemically determined by the expression of neural-specific enolase (NSE; BIOMOL International, Butler Pike Plymouth Meeting, Penn.).

Epithelial Differentiation

For epithelial differentiation, ADSCs were incubated with ATRA (Wako Pure Chemical Industries, Ltd., Osaka, Japan) at a final concentration of 5 μM as previously described by Brzoska et al.[10] The cells incubated without ATRA [the equivalent volume of DMSO (Nacalai Tesque, Kyoto, Japan), solvent for ATRA, was added to the culture] served as a negative control. The medium was replaced every 2 days during a total incubation period of 10 days. Differentiation was immunohistochemically and flow-cytometrically determined by the expression of cytokeratin-18 because of the preferential expression of the "primary" keratins on the intestinal epithelia.

Flowcytometry

Freshly isolated undifferentiated ADSCs (passages 0–3) were stained with unconjugated FITC- or PE-labeled monoclonal antibody (mAb) against CD11b, CD45, or CD90 (CALTAG Laboratories, Invitrogen Corporation, Carlsbad, Calif.), CD31 (Becto-Dickinson, Franklin Lakes, NJ), CD34 (Santa Cruz Biotechnology, Inc. Santa Cruz, Calif.). FITC-labeled goat antimouse IgG (BD Biosciences, San Jose, Calif.) was used as secondary antibody when necessary. In the case of staining with anti-cytokeratin-18 mAb, cells were fixed and permeabilized with Cytofix/Cytoperm solution (BD Biosciences, San Jose, Calif.). The cells thus treated were intracytoplasmically stained with FITC-anti-cytokeratin-18 Ab (PROGEN Biotechnik, Heidelberg, Germany). The stained cells were analyzed by a FACScan (BD Bioscience, San Jose, Calif.).

Measurement of HGF, VEGF, TGF-β, and Adiponectin

ADSCs were cultured in standard 12-well plates until 80% confluence and then culture supernatant was collected. The concentration of HGF (Institute of Immunology Co., Ltd., Tokyo, Japan), VEGF (R&D Systems, Minneapolis, MN), TGF-β (BioSource International, Inc., Camarillo, Calif.), and adiponectin (AdipoGen, Inc., Seoul, Korea) was measured by ELISA according to the manufacturers' instructions.

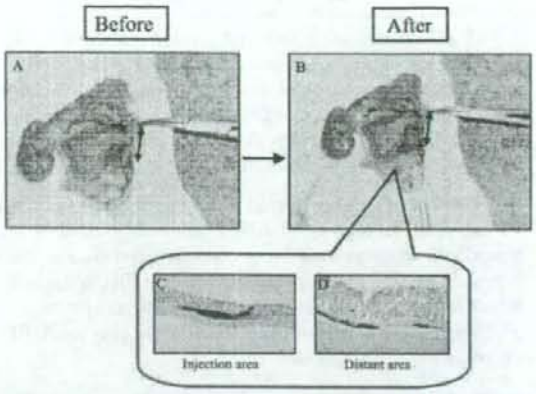

FIGURE 1. Procedure of submucosal injection. A: Under diethyl ether anesthesia, the intestine was exposed by a midline incision of the abdomen (blue arrow indicates the ulcer area injured by the TNBS injection) B: ADSCs or PBS (negative control) were injected from the serosa side into the submucosal layer. C: Using India ink, we confirmed that ADSCs were actually injected into the submucosal layer by this method. D: India ink was found in the submucosal layer of the area distant from the injection point.

In Vivo Examination

Induction of Colitis by TNBS

Colitis was induced by TNBS using the method described previously.[11] Briefly, rats were anesthetized after a 24-hour fast. Then an infant tube (indwelling feeding tube for infants, 4Fr, diameter = 1.35 mm; Atom Medical Co., Tokyo, Japan) was inserted into the anus, and the tip was advanced to 6 cm proximal in the colon. TNBS (Wako Pure Chemical Industries, Ltd., Osaka, Japan) dissolved in 50% ethanol was instilled into the colon through the cannula (30 mg of TNBS in a volume of 0.5 mL). After the instillation, the rats were held upside down by their tails for 60 seconds and then returned to their cages. We prepared more than 40 rats, and colitis was observed in all the rats injected with TNBS. Similarly, rats instilled with PBS served as controls (n = 10). All rats were sacrificed 10 days after administration of TNBS.

Submucosal Injection of ADSCs

ADSCs (passages 0–3), harvested from the culture by trypsin/EDTA solution, were suspended at 10^7 cells in 0.5 mL of PBS containing 2% FBS. Under diethyl ether anesthesia, the intestine was exposed by a midline incision of the abdomen, and ADSCs (10^7 cells) were injected from the serosa into the submucosa of the colon 2 days after the TNBS injection (n = 10; Fig. 1). Rats injected with 0.5 mL of PBS containing

2% FBS served as controls (n = 10).

Furthermore, using India ink, we confirmed that ADSCs were actually injected into the submucosal layer by this method, and India ink was found in the submucosal layer of 9 of the 10 rats injected with India ink (90%). It is noted that no complications were observed after the injection of 0.5 mL of ADSCs or PBS into the submucosa.

Assessment of Inflammation in TNBS-Induced Colitis

To examine the severity of colitis, the body weight of the treated rats was measured every other day, and clinical findings such as area of ulcer (measured using NIH image software on the pictures of colon), length (colocecal junction to anal verge), and weight of the colon 10 days after the TNBS injection were also assessed.

Histological Examination

The tissue specimens were fixed in buffered formalin and embedded in paraffin, and tissue sections were stained by H&E. Colonic inflammation was assessed using modification of the histopathologic grading system of Macpherson and Pfeiffer[12,13]: grade 0 = normal findings; grade 1 = mild mucosal and/or submucosal inflammatory infiltrate (admixture of neutrophils) and edema, punctate mucosal erosions often associated with capillary proliferation, muscularis mucosae intact; grade 2 = grade 1 changes involving 50% of the specimen; grade 3 = prominent inflammatory infiltrate and edema (neutrophils usually predominating), frequently with deeper areas of ulceration extending through the muscularis mucosae into the submucosa, rare inflammatory cells invading the muscularis propria but without muscle necrosis; grade 4 = grade 3 changes involving 50% of the specimen; grade 5 = extensive ulceration with coagulative necrosis bordered inferiorly by numerous neutrophils and lesser numbers of mononuclear cells, necrosis extends deeply into the muscularis propria; grade 6 = grade 5 changes involving 50% of the specimen. All scoring was performed by the same individual under blind conditions.

Measurement of Myeloperoxidase Activity

Tissue myeloperoxidase (MPO) activity was determined by a standard enzymatic procedure as previously described by Krawisz et al[14] with slight modifications. Total protein concentrations of the tissue supernatant and whole-cell lysate were measured using a BCA Protein Assay Kit (PIERCE Co., Rockford, Ill.) for calibration, and myeloperoxidase activity in the tissue homogenate was determined using a Myeloperoxidase Assay Kit (CytoStore Inc., Calgary, Alberta, Canada) according to the manufacturer's instructions.

Measurement of Cytokines in Colonic Tissue

The colonic tissue was homogenized in cold PBS using a Polytron-type homogenizer. Tissue homogenate was then centrifuged at 20,000g for 20 minutes at 4°C to obtain the supernatant. Total protein concentrations of the tissue supernatant and whole-cell lysate were measured using a BCA Protein Assay Kit (PIERCE Co., Rockford, Ill.) for calibration, and protein concentrations of IL-1β (BioSource International, Inc., Camarillo, Calif.), GRO/CINC-1 (functionally equivalent to IL-8; Panafarm Laboratory, Kumamoto, Japan), TNF-α (BioSource International, Inc., Camarillo, Calif.), and IFN-γ (BioSource International, Inc., Camarillo, Calif.) in the tissue homogenate were determined using ELISA kits according to the manufacturers' instructions.

In Situ Cell Proliferation

To evaluate proliferation of the colonic epithelium, 50 mg/kg of 5-bromo-2′-deoxyuridine (BrdU; Wako Pure Chemical Industries, Ltd., Osaka, Japan) was injected intraperitoneally 1 hour before sacrifice, and cells synthesizing DNA were immunohistochemically identified using a BrdU In-Situ Detection Kit (BD Biosciences, San Jose, Calif.) according to the manufacturer's instructions. We then counted the BrdU-positive cells in 10 crypts of the mucosa-bordering ulcer.

Y-Chromosome Fluorescence in Situ Hybridization (Y-FISH)

For assessment of distribution of ADSCs injected into the submucosa, in vivo experiments were performed in sex-mismatched conditions. TNBS-induced colitis models were prepared in female rats, and ADSCs obtained from male rats were injected into the submucosa of the colon in TNBS-induced colitis models. To detect the Y chromosome of ADSCs, we used a STAR-FISH Rat 12/Y Paint (Y FITC; 12 biotin) probe purchased from Cambio (Dry Drayton, Cambridge, UK), and detection protocols were conducted with a Histology FISH Accessory Kit (Dako Cytomation, Dako, Denmark).

Immunofluorescent Staining

Following Y-FISH, colonic tissues in paraffin-embedded sections (3 μm) were stained with mouse mAb against pan-cytokeratin (CHEMICON, now part of Millipore Corporation, Billerica, Mass.), vimentin (Santa Cruz Biotechnology, Inc. Santa Cruz, Calif.), S-100 (COSMO Bio Co., Ltd., Tokyo, Japan) or SMA (Lab Vision Corporation, Fremont, Calif.) after pretreatment procedure (epitope retrieval). They were then stained with PE-labeled goat antimouse IgG antibody (BD Biosciences, San Jose, Calif.). Cellular nuclei were counterstained with DAPI. Images were captured by a LSM510-META and exported as TIFF files and further processed in Adobe PhotoShop.

Statistical Analysis and Ethical Considerations

Results are expressed as mean ± SDs. Differences between groups were examined for statistical significance using the

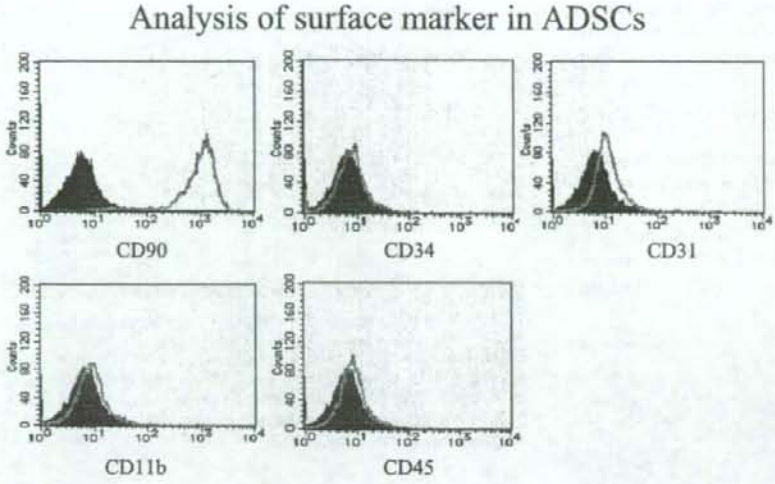

FIGURE 2. Characterization of ADSCs. ADSCs (passage 3) were flow-cytometrically characterized using antibodies against CD11b, CD31, CD34, CD45, and CD90. Cells stained with mAbs are represented by solid pink lines, and those stained with isotype-matched Ig, as negative controls, are represented by green lines. Cells were negative for CD11b, CD34, and CD45 but positive for CD90 and weakly positive for CD31.

Mann-Whitney test. The statistical analysis for the survival rate was performed by log rank test. A P value less than .05 was considered statistically significant. The experimental protocol was approved by the Ethics Review Committee for Animal Experimentation of Kansai Medical University.

RESULTS

Characterization of ADSCs from Subcutaneous Adipose Tissue

ADSCs were flow-cytometrically characterized (after 3 passages) and possible contaminants of hemopoietic lineage cells were excluded. ADSCs were negative for CD11b, CD34, and CD45 but positive for CD90 as shown in Figure 2, indicating that the ADSCs used in our experiments are not in the hemopoietic cell lineages. It is noted that a slight shift in the entire histogram was observed after staining with anti-CD31, indicating that ADSCs seem to be weakly positive for CD31. Furthermore, the doubling time of ADSCs remained unchanged (approximately 36–40 hours) up to 10 passages (Fig. 3). However, their growth stopped at 15 passages.

ADSCs Exhibit Multilineage Potential

We next examined the capacity of ADSCs to differentiate into multilineage cells under the appropriate culture conditions. ADSCs differentiated into adipocytes, osteocytes, neu-

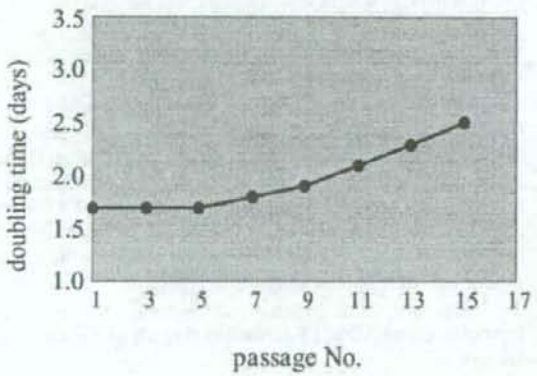

FIGURE 3. Doubling time of ADSCs. Doubling time (day) of ADSCs was determined at the indicated number of passages in DMEM.

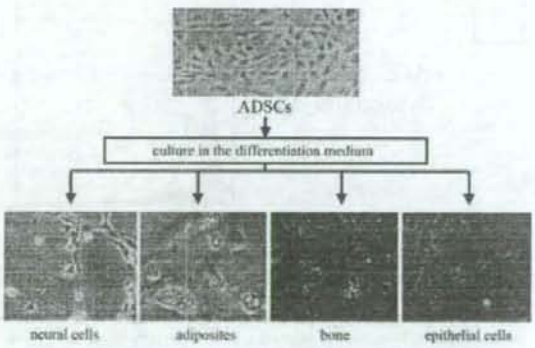

FIGURE 4. Culture of ADSCs. Multilineage differentiation was observed in the appropriate culture condition (bottom). Undifferentiated ADSCs showed multiple layers in the control culture medium.

rogenic cells, and epithelial cells using lineage-specific induction factors. Undifferentiated ADSCs cultured in the medium alone showed multiple layers. Neurogenic differentiation was confirmed by the expression of NSE in the cells with a neuronal morphology (Figs. 4 and 5), and adipogenesis was examined by Oil Red-O staining (Figs. 4 and 5). No lipid droplets stainable with Oil Red-O were observed in undifferentiated ADSCs. Differentiation toward osteocytes was determined by calcification of the extracellular matrix using von Kossa/alkaline phosphatase staining. ADSCs cultured in the epitheliogenic condition (5 μM ATRA for 10 days) showed a morphology resembling epithelial cells (Fig. 4), and they

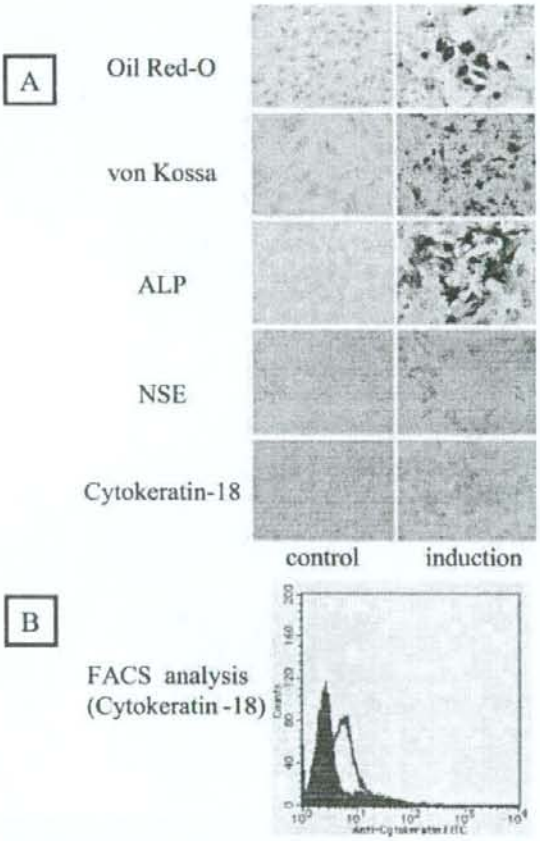

FIGURE 5. Immunohistochemical analyses of ADSCs after differentiation. ADSCs were cultured for 2–4 weeks in adipogenic, osteogenic, neurogenic, or epitheliogenic medium. A: ADSCs thus cultured were stained with Oil Red-O, von Kossa, alkaline phosphatase, NSE, or cytokeratin-18 to identify their differentiation. B: ADSCs cultured with epitheliogenic medium were flow-cytometrically analyzed after staining with FITC-anti-cytokeratin-18 mAb.

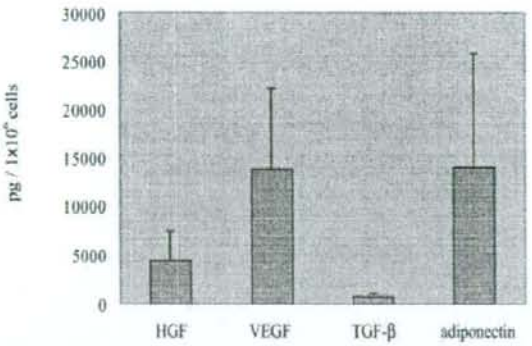

FIGURE 6. Secretion of HGF, VEGF, TGF-β and adiponectin by ADSCs. ADSCs were cultured for 1 week, and the amounts of HGF, VEGF, TGF-β, and adiponectin were measured by ELISA. Columns and bars represent the means ± SDs of 14 samples.

were positive for cytokeratin 18 as shown in Figure 5, where a filamentous cytoskeleton, the typical appearance of epithelial cytokeratins, was stained with this mAb. This was flow-cytometrically confirmed after staining with FITC-anti-cytokeratin-18 mAb (Fig. 5B).

ADSCs Secrete VEGF, HGF, TGF-β, and Adiponectin

The secretion of HGF, VEGF, TGF-β , and adiponectin from ADSCs was examined. They secreted significant amounts of VEGF (13,654 ± 3185 pg/10^6 cells), HGF (4434 ± 1140 pg/10^6 cells), and adiponectin (13,910 ± 5902 pg/10^6 cells) but only minimal amounts (733 ± 136 pg/10^6 cells) of TGF-β (Fig. 6).

Inoculation of ADSCs Reduces Severity of TNBS-Induced Colitis

Changes in body weight, colon weight, and survival rate were evaluated for assessment of the severity of colitis (Fig. 7). There was no statistical significance in the changes in body weight or survival rate between the recipients of ADSCs and the recipients of PBS in TNBS-induced colitis-model rats. However, a significant decrease in colonic weight was observed in the recipients submucosally injected with ADSCs, suggesting that the colonic edema associated with inflammatory responses was ameliorated by the inoculation of ADSCs. Although the results shown in Figure 7 represent only 2 replicate experiments, the values and outcomes in the other experiment were similar to those in Figure 7.

Inoculation of ADSCs Facilitates Repair of Colonic Ulcers

Next, we examined the effects of ADSCs on the repair of colonic ulcers. Eight days after the submucosal injection of ADSCs (or PBS), rats were sacrificed, and the area of colonic